



HAL
open science

A DEM study of the effect of the loss of fine particles on the mechanical behavior of gap-graded soils

Habib Taha, Ngoc-Son Nguyen, Didier Marot, Abbas Hijazi, Khalil Abou-Saleh

► To cite this version:

Habib Taha, Ngoc-Son Nguyen, Didier Marot, Abbas Hijazi, Khalil Abou-Saleh. A DEM study of the effect of the loss of fine particles on the mechanical behavior of gap-graded soils. *Geomechanics for Energy and the Environment*, 2021, 31, pp.100305. 10.1016/j.gete.2021.100305 . hal-04236037

HAL Id: hal-04236037

<https://hal.science/hal-04236037>

Submitted on 10 Oct 2023

HAL is a multi-disciplinary open access archive for the deposit and dissemination of scientific research documents, whether they are published or not. The documents may come from teaching and research institutions in France or abroad, or from public or private research centers.

L'archive ouverte pluridisciplinaire **HAL**, est destinée au dépôt et à la diffusion de documents scientifiques de niveau recherche, publiés ou non, émanant des établissements d'enseignement et de recherche français ou étrangers, des laboratoires publics ou privés.

A DEM study of the effect of the loss of fine particles on the mechanical behavior of gap-graded soils

Habib Taha^{a,b}, Ngoc-Son Nguyen^{a,*}, Didier Marot^a, Abbas Hijazi^b, Khalil Abou-Saleh^b

^a*GeM Institute, University of Nantes, 58 rue Michel Ange, BP 420, 44606, Saint-Nazaire Cedex, France*

^b*MPLAB-Multidisciplinary Physics Laboratory, Faculty of Sciences, Lebanese University, Hadat-Baabda, Lebanon*

Abstract

Modelling of suffusion in granular soils by using a fully coupled fluid-DEM model is still challenging due to its very high cost of computation. The particle removal approach is an alternative to mimic the erosion of fine particles by the seepage flow. In this paper, we study different particle removal methods and their impact on the mechanical behavior of eroded samples. Gap-graded samples with different fine contents f_c were simulated by using the DEM. Fine particles are removed from the original sample under constant stress state by using three different methods: random removal, the method of Scholtès et al. based on the particle internal moment m^p , and a new method proposed here that is based on the concept of weak and strong force networks. A micro-mechanical investigation into numerical samples shows that the fine particles have small contribution in carrying stresses when $f_c \leq 30\%$ but they offer a great bracing effect to the coarse fraction, which allows the latter to carry high stresses. As a result, a removal of fine particles destroys greatly this bracing system, leading to a great reduction in the bearing capability of the coarse fraction. A comparison between the three methods shows that a removal of fine particles belonging to the weak force network has a lower impact on the mechanical behavior of eroded samples than the random removal. In addition, the method of Scholtès et al. gives results quite similar to those given by the random removal in terms of the shear strength of eroded samples.

Keywords: Discrete element method, Suffusion, Gap-graded soils, Particle removal, Force network

1. Introduction

Internal erosion can occur through the embankment and/or the foundation of earth structures such as dams and dikes. This phenomenon is caused by the water seepage that can detach soil's particles and transport them out of the structure when the hydraulic forces are sufficiently high. Suffusion is a particular

*Corresponding author

Email addresses: habib.taha@univ-nantes.fr (Habib Taha), ngocson.nguyen@univ-nantes.fr (Ngoc-Son Nguyen), didier.marot@univ-nantes.fr (Didier Marot), abhijaz@ul.edu.lb (Abbas Hijazi), kabousaleh@ul.edu.lb (Khalil Abou-Saleh)

form of internal erosion, which is described by a migration of soil's finer particles through the void space of the solid skeleton composed of soil's coarser particles. Granular soils with gap-graded or upwardly concave grain size distribution [21, 29] might be susceptible to suffusion. Due to migration of finer particles, the compactness and micro-structure of the eroded soil change [15], leading to a potential degradation of the mechanical properties of the eroded soil. Knowledge of consequences of suffusion on the mechanical behavior of suffusive soil is then of paramount importance to assess the mechanical stability of earth structures.

Several experimental studies tackled effects of suffusion on the mechanical behavior of eroded soils. Sterpi [24] performed first suffusion tests on samples of sand and gravel and then reconstituted samples with the same particle size gradations as those of the eroded samples to investigate the mechanical behavior of the eroded soil by means of triaxial tests. The author found a significant increase in shear strength with loss of fine particles. Chen et al. [5] studied the behavior of eroded soils by replacing a fraction of fine particles in the original samples by salt having the same particle size distribution as that of the replaced particles. Water was then injected to saturate the samples and dissolve completely the salt before performing triaxial tests. This study showed that the mechanical behavior of the tested soil is strongly degraded by the dissolution of the salt. It is worth noting that suffusion is a complex phenomenon that comprises detachment, transport and potential filtration of fine particles, and none of the two above methods can fully represent the soil's micro-structure after suffusion. Aboul Hosn et al. [8] froze eroded samples after suffusion tests to set them in a triaxial device, and then unfroze them before performing drained and undrained tests. The authors found that the eroded samples become more dilatant; however, their shear strength can be higher or lower than that of the non-eroded samples depending on their initial density. Some triaxial erosion apparatuses have been recently developed by Chang and Zhang [2] and by Ke and Takahashi [11] to perform first seepage tests and then triaxial tests on the same sample without any disturbance. These studies concluded that suffusion leads to a significant reduction in dilatancy and shear strength of eroded soils. A consensus on effects of suffusion on the mechanical properties of eroded soils has not been reached yet. More future researches need to be carried out to shed light on this subject.

Numerical models have been developed as complementary tools to investigate the behavior of eroded soils. Rousseau et al. [20] proposed a continuum-based elasto-plasticity model, and Hicher et al. [7] proposed a homogenization-based model where a granular soil is viewed as a set of contact planes with various orientations. Both approaches take into account only an increase in porosity due to suffusion and predict a reduction in shear strength and dilatancy of eroded soils. Discrete element method (DEM) can also be used to model the behavior of eroded soils. The key point in this kind of models is how to produce the internal state of the eroded soil. An ideal way is to couple the DEM to a CFD method (Computational Fluid Dynamics) to model finely the fluid flow within the pores between solid particles such as LBM (Lattice Boltzmann Method) or SPH (Smoothed Particle Hydro-dynamics) [6, 13, 19, 26]. However, these fully coupled DEM-CFD models require a huge computational effort. To significantly reduce the computation

time, some authors proposed to model the fluid flow through a granular medium by using locally averaged quantities such as fluid velocity and pressure over a pore [4] or a fluid cell whose size is several times larger than the averaged particle diameter [32]. However, these models are still costly to simulate the full process of suffusion. It is worth mentioning that numerical simulation of gap-graded or widely graded soils by using the DEM without water flow is already very costly since a great number of particles is required to fulfill the conditions for a RVE (Representative Volume Element). If the water flow model is added to simulate the whole suffusion process including detachment, transport and filtration of finer particles, the computational cost becomes extremely high. Therefore, these coupled DEM-CFD models have been almost used to simulate only the onset of suffusion [1, 9, 10].

An alternative approach to produce the internal state of an eroded sample with the DEM consists in removing a certain fraction of finer particles from the original sample [22, 30, 31] to mimic the loss of finer particles caused by suffusion. Wood et al. [30, 31] remove a fraction of finest particles from the original sample subjected to a given stress state, while Scholtès et al. [22] take into consideration the internal moment considered as the degree of interlocking of each particle in addition to its size. It is worth mentioning that this removal particle approach is quite similar to the experimental technique of Chen et al. [5] based on the salt dissolution mentioned above. This approach was found to be capable of reproducing the reduction in dilatancy and shear strength caused by suffusion. As stated by Kenney and Lau [12], a granular soil is composed of a *primary fabric* or *solid skeleton* that supports primarily overburden stresses and a fraction of *loose particles* which are contained within the primary fabric and do not bear significantly stresses. If the hydraulic forces are sufficiently high, and the loose particles are sufficiently smaller in size than the *controlling constriction size* of the solid skeleton (the largest diameter of loose particles that can pass through the solid skeleton), then water flow can wash out these loose particles from the solid skeleton. In this case, the removal particle approach might be suitable to represent the internal state of eroded soils. For the soils that exhibit important clogging effect, i.e., detached particles might be retained by the solid skeleton, the DEM needs to be coupled to a model to access filtration of erodible particles. For instance, according to Aboul-Hosn [1], a fine particle can be transported through the whole interstitial space of the solid skeleton and then can be removed from the sample if its diameter is smaller than the controlling constriction size of the solid skeleton. The latter parameter can be determined by using the constriction size distribution of the solid skeleton [16, 23]. It is worth mentioning that suffusion is such a complex process that a simple removal of fine particles cannot represent all mechanisms occurring during this process: rather, it gives a first approximation of the internal state of an eroded soil. However, this approach allows us to take into account the loss of fine particles and the associated rearrangement of the microstructure of eroded soils, which are two of the most important mechanisms induced by suffusion.

In this paper, we adopt the particle removal approach to model eroded soils with the DEM. We aim to study how the behavior of eroded samples depends on the way that fine particles are removed. Three

different particle removal strategies are studied. Firstly, fine particles are randomly removed. Secondly, fine particles are chosen depending on their size and their degree of interlocking by using the criterion of Scholtès et al. [22]. Thirdly, we introduce a new method based on the concept of *weak and strong force chains* introduced by Radjai et al. [18] to separate the loose particles from those of the solid skeleton. Triaxial tests are performed on non-eroded and eroded gap-graded samples composed of spherical particles. The behaviors of samples eroded by the three particle removal methods are compared. A micro-mechanical investigation is also carried out to explain macroscopic observations.

This paper is organized as follows. The numerical samples considered in this study are first presented. Next, consequences of the loss of fine particles caused by the random removal method on the mechanical behavior of these samples are analyzed at the macro- and micro-scales. Two methods to identify the loose particles are then presented: the method of Scholtès et al. and the one based on the force networks. Finally, these three methods are compared in terms of mechanical behavior of resulting eroded samples.

2. Numerical samples

The numerical samples presented in this paper are composed of spherical particles and have a gap-graded particle size distribution (PSD) shown in Figure 1 with a gap-ratio $G_r = D_{\min}/d_{\max} = 3$ (D_{\min} is the minimum diameter of the coarse fraction and d_{\max} is the maximum diameter of the fine fraction). Fine content f_c , defined as the ratio of the mass of all the fine particles to the total solid mass, of the simulated mixtures is varied from 0% to 40% with a step of 5%. These samples are simulated by using the DEM open-source software YADE [28]. The numerical model used for these samples and the procedures for the sample preparation and for the triaxial test were detailed in our previous paper [25]. The parameters used in the model are: normal particle stiffness $k_n/D = 250$ MPa, stiffness ratio $k_t/k_n = 0.5$ and friction angle $\varphi = 35^\circ$.

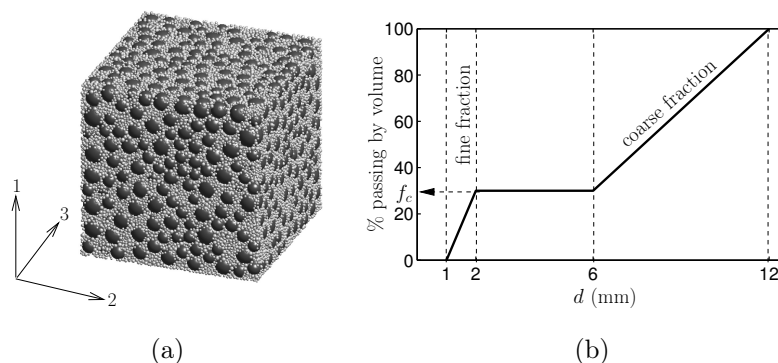


Figure 1: (a) A simulated granular mixture and (b) the considered gap-graded grain size distribution.

The particles were first generated into a parallelepiped box composed of six rigid walls. They were then compacted to obtain the densest state and subjected to triaxial loading. Their mechanical behavior was analyzed at the macro-scale as well as at the micro-scale in [25]. Table 1 summarizes some characteristics of the simulated samples. The number of particles for each sample was chosen such that it is sufficiently high to guarantee the representativity of the simulated sample but it is not too high to keep the computation time reasonable. It should be noted that, for gap-graded samples, a higher fine content f_c requires a bigger number of particles. For instance, 16 663 particles were used for the sample with $f_c = 5\%$, while 116 610 particles were used for the sample with $f_c = 30\%$. The representativity of the simulated samples was already discussed in [25]. The rigidity of the particles is assessed by computing the relative overlap γ of each particle, which is the ratio of its maximum overlap with its neighbors to its diameter. Table 1 shows that, with the chosen value of the normal particle stiffness $k_n/D = 250$ MPa, the overlaps between particles are relatively small with a mean relative overlap smaller than 0.1% and a maximum value smaller than 2.2%. It can be seen that the global void ratio e (defined as the ratio of the void volume to the total solid volume) decreases as fine content f_c increases and reaches its minimum value at $f_c = 30\%$ (more precisely, this optimum fine content is 32% as shown in [25]); above this optimum fine content, e increases with an increase in fine content. The densities of the coarse and fine fractions are described by the intergranular and interfine void ratios, e_c and e_f , respectively:

$$e_c = \frac{V_v + V_s^f}{V_s^c} = \frac{e + f_c}{1 - f_c}, \quad e_f = \frac{V_v}{V_s^f} = \frac{e}{f_c}, \quad (1)$$

where V_v is the void volume, and V_s^c and V_s^f are the respective solid volumes of the coarse and fine fractions. As fine content f_c increases, e_c increases while e_f decreases, meaning that the coarse fraction gets looser, while the fine fraction gets denser. More interestingly, both e_c and e_f reach almost the same value at the optimum fine content of 30%. As fine content f_c increases, the macroscopic friction angle ϕ_{peak} calculated by using the Mohr-Coulomb yield criterion at the peak state is found to increase, then reaches the highest value at the optimum fine content of 30%, and finally decreases when $f_c > 30\%$. On the other hand, fine content has a negative effect on the macroscopic friction angle ϕ_{critical} at the critical state. Indeed, ϕ_{critical} decreases as fine content f_c increases up to 35% since a higher fine content leads to a stronger dilatancy, and then a stronger softening phase.

According to Chang and Zhang [3], a gap-graded soil with gap ratio $G_r \geq 3$ might be unstable – in other words, fine particles might migrate due to seepage flow. In this context, the study of the mechanical behavior of gap graded soils with $G_r = 3$ which corresponds actually to the boundary between unstable and stable states appears particularly interesting. Indeed, Chang and Zhang [3] showed that some gap-graded soils with $G_r = 3$ are stable, while other ones are unstable. The coarse fraction of each gap-graded sample simulated here has a uniform PSD from $D_{\min} = 6$ mm to $D_{\max} = 12$ mm with $D_{15} = 6.9$ mm (diameter corresponding to 15% by mass of the coarse particles). For samples of spherical particles with uniform PSDs,

Table 1: Number of particles N , sample size L/D_{\max} , the mean and maximum relative overlaps $\bar{\gamma}$ and γ_{\max} , global void ratio e , intergranular void ratio e_c , interfine void ratio e_f , the macroscopic friction angles, ϕ_{peak} and ϕ_{critical} , at the peak and critical states, respectively, for different values of fine content f_c .

f_c (%)	0	5	10	15	20	25	30	35	40
N	6000	16 663	31 643	49 907	70 012	94 608	116 610	124 641	142 411
L/D_{\max}	11.7	7.3	7.2	7.2	7.2	7.3	7.4	7.2	7.2
$\bar{\gamma}$ (%)	0.08	0.08	0.09	0.1	0.12	0.09	0.07	0.07	0.07
γ_{\max} (%)	0.5	0.33	0.48	1.6	2.2	0.8	0.44	0.9	0.7
e	0.6	0.54	0.46	0.4	0.33	0.29	0.28	0.3	0.32
e_c		0.62	0.63	0.64	0.66	0.72	0.83	1.0	1.2
e_f		11.5	4.6	2.8	2.6	1.6	0.95	0.85	0.79
ϕ_{peak} ($^\circ$)	28	28	29	30	33	37	40	37	36
ϕ_{critical} ($^\circ$)	21	20	22	19	21	17	15	11	15

the maximum and minimum void ratios, e_{\max} and e_{\min} , are around 0.69 and 0.56, respectively [16]. The values of the intergranular void ratio e_c shown in Table 1 indicate that the coarse fraction in the simulated gap-graded samples is at relatively loose state. Therefore, the controlling constriction size D_c^* for the coarse fraction of these samples can be estimated as $D_c^* = 0.25D_{15} = 1.73$ mm according to Nguyen et al. [16]. This indicates that some fraction of fine particles with diameters smaller than 1.73 mm might migrate through the void space between the coarse particles. It should be noted that gap-graded soils become more erodible at higher gap-ratio G_r ; however, a higher value of G_r leads to a larger number of particles and then to a very long computation time. As our aim is to study consequences of the loss of fine particles on the mechanical behavior of gap-graded soils rather than their erodibility, $G_r = 3$ was chosen here to keep the computation time reasonable.

In the following, we present three different strategies to erode the above samples by removing a fraction of fine particles from them. For the first strategy, fine particles are randomly removed, while for the two other strategies, only the loose ones that do not carry significant stresses are removed. The behavior of the eroded samples is analyzed at the macro- and micro-scales. Throughout this paper, the particle removal is performed at the isotropic stress state. The influence of the stress state at which fine particles are removed on the behavior of eroded samples was studied by Scholtès et al. [22], and thus is not studied here. We rather focus our study on the influence of the strategy used to remove fine particles.

3. Random removal of fine particles

For this particle removal strategy, a fraction of fine particles are randomly removed from the original sample at a given stress state. In fact, this method is inspired from the experimental technique used by Chen et al. [5] who replaced a fraction of fine particles by salt, and then dissolved salt by injecting water into samples. Wood et al. [30, 31] and Scholtès et al. [22] removed fine particles one by one and stabilized the sample each time a particle is removed; as a result, this removal process is very time-consuming. To remove a given mass fraction μ_e of fine particles (called as eroded mass), we remove instead a package of fine particles with partial mass fraction $\Delta\mu_e$ at each step and stabilize the sample by performing a sufficient number of computation cycles to bring the sample to the equilibrium under constant stress state. The sample is considered to be at the equilibrium if the average magnitude of the resultant forces acting on the particles is 100 times smaller than the average magnitude of the contact forces. This removal process is repeated until we reach the target removed mass fraction μ_e . It is worth mentioning that the total and partial removed mass fractions μ_e and $\Delta\mu_e$ are defined as the ratio of the solid mass of the removed fine particles to the total solid mass of the original sample. The partial fraction $\Delta\mu_e$ of fine particles removed at each removal step can be thought of as being the erosion rate. Indeed, to erode experimentally the same mass from a sample in a hydraulic gradient controlled condition, we can apply a high hydraulic gradient during a short duration to erode quickly the sample but we can also erode slowly the sample by applying a moderate hydraulic gradient during a longer duration.

3.1. Influence of the removal rate $\Delta\mu_e$

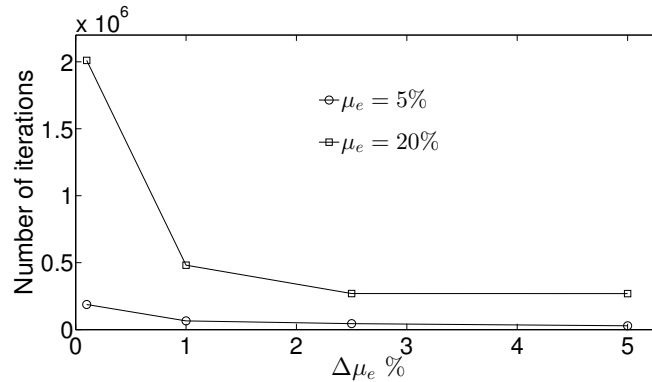


Figure 2: Number of iterations versus removal rate $\Delta\mu_e$ to remove 5% and 20% of the solid mass from the sample of $f_c = 30\%$.

To study the effect of the removal rate $\Delta\mu_e$ on the behavior of the eroded sample, we erode the sample with $f_c = 30\%$ at different rates $\Delta\mu_e$ in order to reach eroded masses $\mu_e = 5\%$ and 20% . This sample is chosen since its fine fraction plays an important role in its mechanical behavior. It should be noted that the number of removal steps decreases with an increase in the removal rate $\Delta\mu_e$; however, the number of

computation cycles (iterations) needed for each removal step to stabilize the sample might increase as the sample is more disturbed with higher removal rate. Figure 2 shows the total number of iterations needed to remove 5% and 20% of the solid mass with different removal rates $\Delta\mu_e$. It can be seen that the computation cost is quite high when a very small removal rate $\Delta\mu_e$ is used and it decreases greatly with an increase in $\Delta\mu_e$. Moreover, an increase in $\Delta\mu_e$ above 1% does not lead to a gain in the computation time.

Figure 3 shows the stress ratio q/p ($q = \sigma_{11} - \sigma_{33}$ is the deviatoric stress and $p = (\sigma_{11} + 2\sigma_{33})/3$ is the mean stress) and the volumetric strain ε_v during the triaxial loading for the original samples with $f_c = 20\%$ and 30% and the corresponding eroded samples with eroded mass $\mu_e = 20\%$ obtained at different removal rates $\Delta\mu_e$. It can be seen that a higher value of $\Delta\mu_e$ induces a greater fluctuation of the stress-strain curve of eroded samples. However, the removal rate $\Delta\mu_e$ has a negligible effect on the mechanical behavior of the eroded samples. As no significant gain in computation time is observed for a removal rate $\Delta\mu_e$ above 1%, we choose $\Delta\mu_e = 1\%$ in the following analyses.

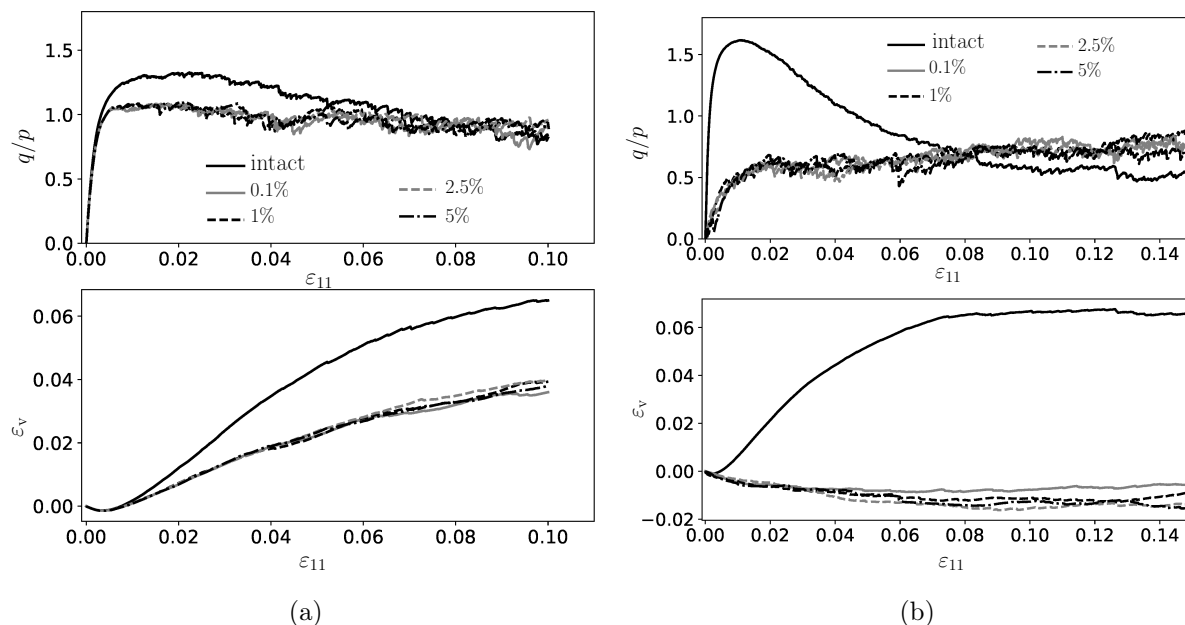


Figure 3: Stress-strain behavior of the intact samples and of the samples eroded with eroded mass $\mu_e = 20\%$ and with different removal rates $\Delta\mu_e$: (a) for $f_c = 20\%$ and (b) for $f_c = 30\%$.

3.2. Macroscopic investigation

The above procedure is used here to erode the samples with initial fine contents $f_c = 10\%$, 20% and 30%. Table 2 shows the void ratios and the maximum stress ratio $(q/p)_{\max}$ for the original soils and the eroded ones with different eroded masses μ_e . It can be seen that a removal of fine particles from the original soils leads obviously to an increase in the interfine void ratio e_f , and thus an increase in the global void ratio e . However, the intergranular void ratio e_c remains almost unchanged except for the initial fine content

Table 2: Void ratios e , e_c and e_f and the maximum stress ratio $(q/p)_{max}$ of the samples eroded from the original ones with $f_c = 10\%$, 20% and 30% and with different eroded masses μ_e .

μ_e	$f_c = 10\%$				$f_c = 20\%$				$f_c = 30\%$			
	e	e_c	e_f	$(q/p)_{max}$	e	e_c	e_f	$(q/p)_{max}$	e	e_c	e_f	$(q/p)_{max}$
0	0.50	0.67	5.0	1.20	0.35	0.69	1.75	1.30	0.29	0.84	0.95	1.60
5%	0.58	0.67	11.0	1.19	0.42	0.69	2.67	1.26	0.35	0.83	1.34	1.28
10%	0.67	0.67	-	1.17	0.50	0.69	4.5	1.14	0.43	0.83	1.91	1.13
15%	-	-	-	-	0.59	0.69	10.0	1.11	0.51	0.83	2.90	0.78
20%	-	-	-	-	0.69	0.69	-	1.06	0.57	0.81	4.30	0.80

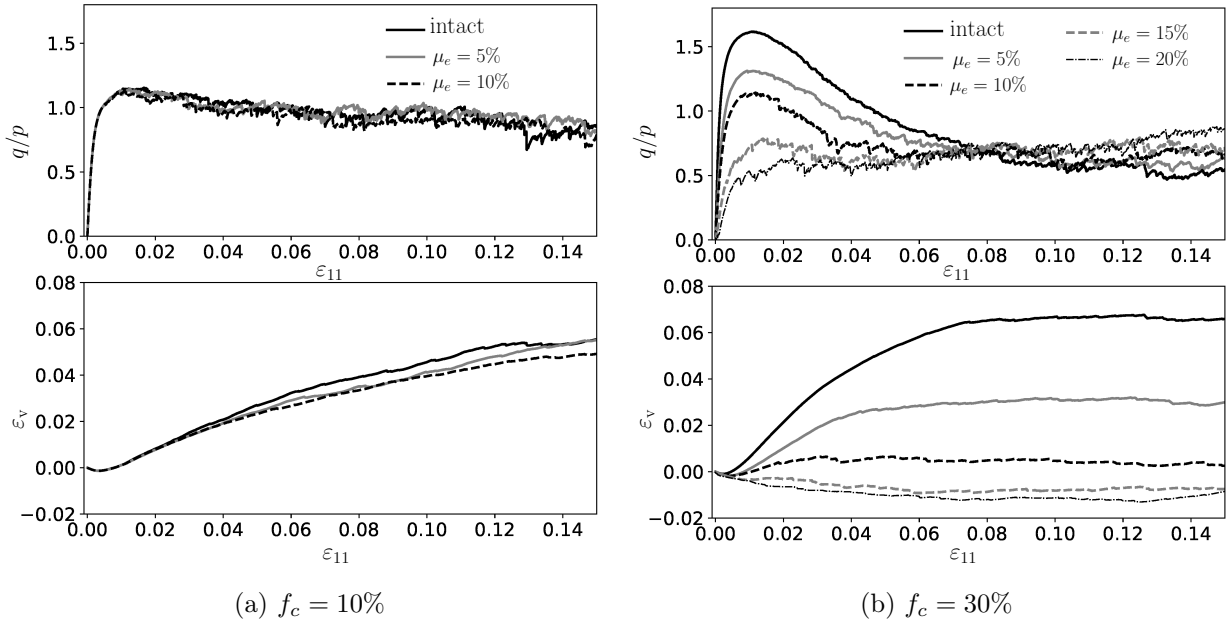


Figure 4: Stress-strain behavior of the original samples and of the eroded samples with different percentages μ_e after random removal of fine particles: (a) for $f_c = 10\%$ and (b) for $f_c = 30\%$.

$f_c = 30\%$ for which a slight decrease in e_c is observed due to the contraction during the removal process as mentioned previously. Figure 4 shows the behavior of the intact samples with $f_c = 10\%$ and 30% and of the corresponding eroded samples with different eroded masses μ_e . It can be seen that a removal of fine particles causes a very little effect to the behavior of the sample with fine content $f_c = 10\%$ (Figure 4.a) but a great effect to the behavior of the samples with $f_c = 30\%$ (Figure 4.b). Indeed, with 10% of the eroded mass, the sample with $f_c = 30\%$ loses about 30% of its shear strength and becomes much less dilatant (Figure 4.b). In addition, with 20% of the eroded mass, the eroded sample has the same fine content as that of the original sample with $f_c = 10\%$ but the former is much less resistant and dilatant than the latter. Table 2 shows clearly that the effect of the loss of fine particles on the mechanical behavior of gap-graded soils

is more accentuated for a higher value of the initial fine content. With the same eroded mass of 15%, the sample with $f_c = 20\%$ loses actually about 14% of its shear strength, while the sample with $f_c = 30\%$ loses half of its shear strength.

The above results are qualitatively in good agreement with the experimental results obtained by Chen et al. [5]. This experimental study showed that the shear resistance and the dilatancy of gap-graded soils decrease greatly with a loss of fine particles. With the same amount of loss of fine particles, the decrease in the shear strength is more marked for the soils with an initial fine content of 35% than for those with an initial fine content of 20%. In the following, we present an investigation at the particle scale to explain the above macroscopic observations.

3.3. Microscopic investigation

To study the microstructure of a gap-graded soil, three different coordination numbers \mathcal{N}_C^{C-C} , \mathcal{N}_F^{F-F} and \mathcal{N}_C^{C-F} were used by Taha et al. [25] to describe, at the micro-scale, the densities of the coarse fraction, of the fine fraction and of the interface between them, respectively. \mathcal{N}_C^{C-C} and \mathcal{N}_C^{C-F} are the respective average numbers of contacts between coarse particles ($C-C$) and between coarse and fine particles ($C-F$) per coarse particle (C); and \mathcal{N}_F^{F-F} is the average number of contacts between fine particles ($F-F$) per fine particle (F). Table 3 shows values of \mathcal{N}_C^{C-C} , \mathcal{N}_C^{C-F} and \mathcal{N}_F^{F-F} for the original samples with $f_c = 10, 20$ et 30% and the corresponding eroded samples with different eroded masses μ_e . Almost zero values of \mathcal{N}_C^{C-F} and \mathcal{N}_F^{F-F} for the original sample with $f_c = 10\%$ indicate that the fine particles are floating within the voids between coarse particles and do not carry significant stresses. At this fine content, the coarse particles constitute the primary fabric to carry mainly stresses; therefore, a loss of fine particles does not induce any effect to its mechanical behavior. For a fine content of 20%, a small fraction of fine particles are intercalated between coarse particles but most of them are still floating within the void of the primary fabric. As a result, a small disturbance to the primary fabric is induced when fine particles are removed. At 30% of fine content, which is the optimum fine content, fine particles fill greatly the void between the coarse particles; some of them separate coarse particles, leading to a decrease in \mathcal{N}_C^{C-C} . At this fine content, fine particles are in contact with each other ($\mathcal{N}_F^{F-F} = 2.2$); and coarse particles are greatly surrounded by fine particles ($\mathcal{N}_C^{C-F} = 44.9$). A removal of fine particles causes a strong degradation to the fine fraction and its interface with the coarse one: \mathcal{N}_C^{C-F} and \mathcal{N}_F^{F-F} decrease strongly with an increase in the eroded mass μ_e and they become almost insignificant from $\mu_e = 15\%$ ($\mathcal{N}_C^{C-F} = 4.2$ and $\mathcal{N}_F^{F-F} = 0.1$). It is also interesting to note that although a contraction occurs during the particle removal process, \mathcal{N}_C^{C-C} slightly decreases with the loss of fine particles, meaning that the coarse fraction is also slightly degraded.

The degradation caused to the granular microstructure by a removal of fine particles affects greatly the transmission of stresses through fine and coarse particles. To study this effect, we quantify the contributions of the fine and coarse fractions towards carrying the macroscopic stress σ by the following partial stress

μ_e	$f_c = 10\%$			$f_c = 20\%$			$f_c = 30\%$		
	\mathcal{N}_C^{C-C}	\mathcal{N}_C^{C-F}	\mathcal{N}_F^{F-F}	\mathcal{N}_C^{C-C}	\mathcal{N}_C^{C-F}	\mathcal{N}_F^{F-F}	\mathcal{N}_C^{C-C}	\mathcal{N}_C^{C-F}	\mathcal{N}_F^{F-F}
0	4.7	0.0	0.0	4.6	0.4	0.0	3.8	44.9	2.2
5%	4.7	0.0	0.0	4.6	0.4	0.0	3.8	21.8	0.7
10%	4.7	-	-	4.6	0.2	0.0	3.7	11.8	0.3
15%	-	-	-	4.6	0.1	0.0	3.2	4.2	0.1
20%	-	-	-	4.6	-	-	3.2	1.3	0.1

Table 3: Coordination numbers \mathcal{N}_C^{C-C} , \mathcal{N}_C^{C-F} and \mathcal{N}_F^{F-F} for different percentages μ_e of fine particles removed from the original samples with $f_c = 10\%$, 20% and 30% at the initial state.

tensors $\hat{\sigma}^F$ and $\hat{\sigma}^C$:

$$\hat{\sigma}_{ij}^F = \frac{1}{V} \sum_{p \in F} M_{ij}^p, \quad \hat{\sigma}_{ij}^C = \frac{1}{V} \sum_{p \in C} M_{ij}^p, \quad (2)$$

where the superscript p runs over the set of fine particles (F) for $\hat{\sigma}^F$ and the set of coarse particles (C) for $\hat{\sigma}^C$. The tensor M^p , called *internal moment tensor* by Moreau [14], is defined for each particle p as follows:

$$M_{ij}^p = \sum_{k \in p} f_i^k r_j^k \quad (3)$$

where the superscript k runs over all the contacts on the particle under consideration; the vector r^k connects the particle center to the contact point; and f^k is the contact force vector. With some developments, one can obtain $\sigma = \hat{\sigma}^F + \hat{\sigma}^C$ (see [25]). From the tensors $\hat{\sigma}^F$ and $\hat{\sigma}^C$, the partial mean stresses, \hat{p}^F and \hat{p}^C , and the partial deviatoric stresses, \hat{q}^F and \hat{q}^C , carried by the respective fine and coarse fractions can be computed as follows:

$$\begin{cases} \hat{p}^F = (\hat{\sigma}_{11}^F + 2\hat{\sigma}_{33}^F)/3, & \hat{p}^C = (\hat{\sigma}_{11}^C + 2\hat{\sigma}_{33}^C)/3, \\ \hat{q}^F = \hat{\sigma}_{11}^F - \hat{\sigma}_{33}^F, & \hat{q}^C = \hat{\sigma}_{11}^C - \hat{\sigma}_{33}^C. \end{cases} \quad (4)$$

Figure 5 shows the contributions of the fine and coarse fractions to the macroscopic mean and deviatoric stresses (\hat{p}^F and \hat{q}^F for the fine fraction, and \hat{p}^C and \hat{q}^C for the coarse fraction) during the triaxial loading for the two original samples with $f_c = 20\%$ and 30% and for their corresponding eroded samples with eroded mass $\mu_e = 10\%$. Figure 5.a confirms that, at 20% of fine content, the fine particles have no significant contributions towards carrying stresses. However, a loss of fine particles leads to a visible reduction in stresses carried by the coarse fraction, particularly the deviatoric stress \hat{q}^C . This result means that although the fine particles do not contribute greatly towards carrying stresses, they serve as a bracing system to laterally stabilize the solid skeleton mainly constituted of coarse particles, allowing them to carry high stresses. A degradation or destruction of this bracing system causes a reduction in the capability of the

coarse fraction to carry the shear stress, hence a reduction in the shear strength of the sample. This bracing effect offered by the fine fraction is more marked for the sample with 30% of fine content (Figure 5.b). At this fine content, the fine fraction is more stressed, and thus gives a higher bracing effect, allowing the coarse fraction to carry much higher deviatoric stress than at 20% of fine content. In addition, only 10% of mass loss causes a great degradation to the fine fraction, which leads, in turn, to a strong reduction in the deviatoric stress carried by the coarse fraction.

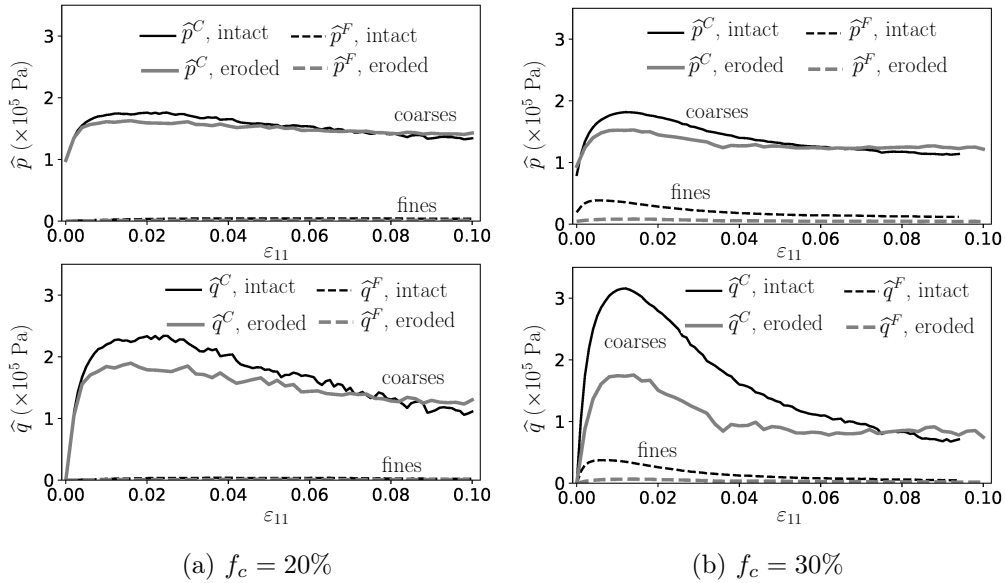


Figure 5: Partial mean and deviatoric stresses of the coarse fraction (\hat{p}^C and \hat{q}^C) and of the fine fraction (\hat{p}^F and \hat{q}^F) versus axial strain ε_{11} for the intact samples (black curves) with original fine contents of 20% (a) and 30% (b) and for the corresponding eroded samples (gray curves) with the same eroded mass $\mu_e = 10\%$.

Figure 6 shows reduction of the partial mean and deviatoric stresses carried by the fine fraction (\hat{p}^F and \hat{q}^F) and the coarse fraction (\hat{p}^C and \hat{q}^C) at the peak state versus the mass loss μ_e for the samples with $f_c = 20$ and 30%. It is clearly shown that the deviatoric stress \hat{q}^C carried by the coarse fraction decreases slightly with the mass loss μ_e for $f_c = 20\%$ but strongly for $f_c = 30\%$. In addition, the mean stress \hat{p}^C carried by the coarse fraction is much less impacted by the loss of fine particles than the deviatoric stress \hat{q}^C . The reduction in the capability of the coarse fraction in carrying the shear stress, due to a loss of the bracing effect offered by the fine fraction, explains why the eroded soils lose their shear strength, particularly for those at high fine content.

Stress transmission through a granular material is well known to be strongly heterogeneous. With a fine content of 30%, the fine particles carry only about 10% of the macroscopic deviatoric stress. In addition, among the fine particles, some carry high stresses, other carry very little or no stresses. It is logic to think that the seepage flow cannot detach the fine particles that are highly stressed by other particles. The

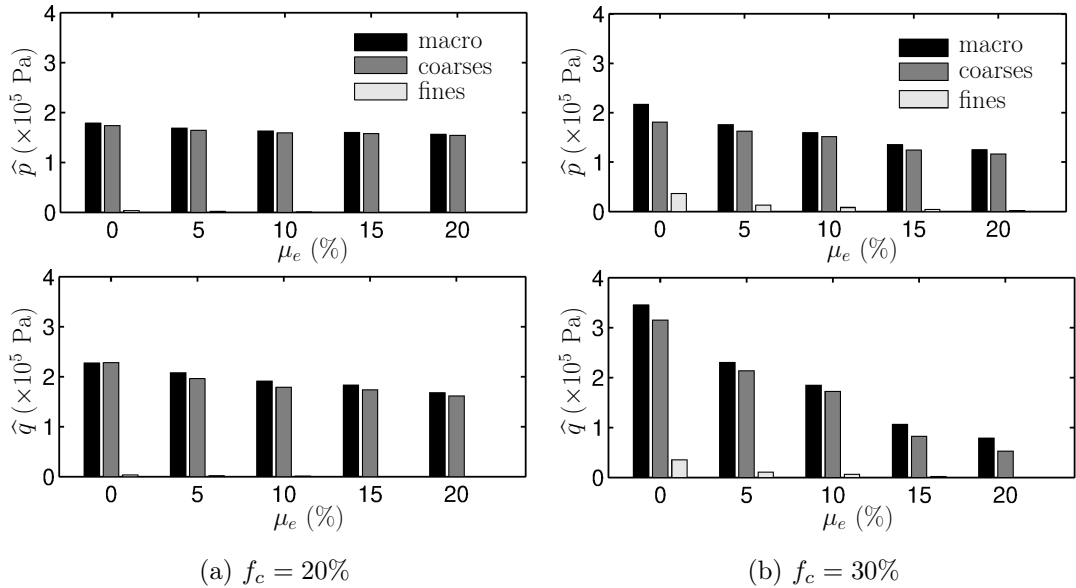


Figure 6: Macroscopic mean and deviatoric stresses p and q , and those carried by the fine fraction (\hat{p}^F and \hat{q}^F) and the coarse fraction (\hat{p}^C and \hat{q}^C) versus the mass loss μ_e at the peak state for two samples with (a) $f_c = 20\%$ and (b) $f_c = 30\%$.

interlocking between particles is an important factor that affects the susceptibility of particles to internal erosion. Indeed, Kenney and Lau [12] stated that a granular soil possesses a *primary fabric*, also called *solid skeleton*, that supports primarily stresses and a fraction of *loose particles* that are located within the pores of this primary fabric and do not support significantly stresses. The primary fabric is hardly eroded, while the loose particles are susceptible to be detached by the seepage flow. At a significant high content, fine particles can take part in the primary fabric. Therefore, a random removal of fine particles from a given original soil is not adequate to produce the internal state of a soil after erosion as fine particles of the primary fabric are also removed. A particle removal procedure should be applied only on the loose fraction. The key point here is how these loose particles are identified. In the next section, we will present two methods to identify them. The first method proposed by Scholtès et al. [22] relies on the internal moment tensor \mathbf{M}^p defined for each particle (see Equation (3)). We propose also a new method based on a separation of the particles belonging to the strong force network from those belonging to the weak force network. The mechanical behavior of the samples eroded by these two methods are compared to each other and to that obtained with the random removal method presented above.

4. Removal of loose fine particles

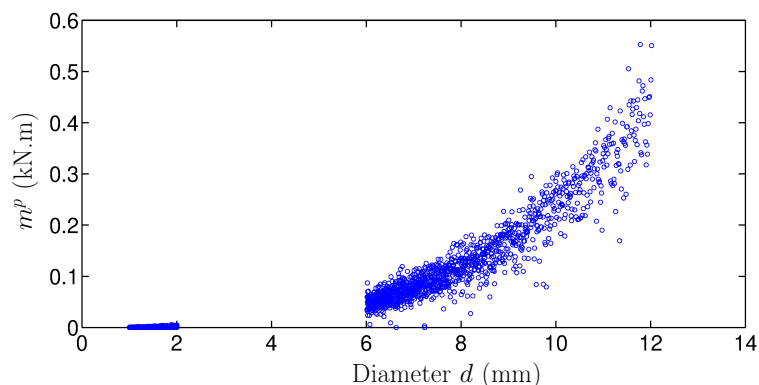
4.1. Method based on the internal moment tensor \mathbf{M}^p

The internal moment tensor \mathbf{M}^p was defined in Equation (3). It can be thought of as being the contribution of each particle to the macroscopic stress $\boldsymbol{\sigma}$ as the latter can be found by summing \mathbf{M}^p over all

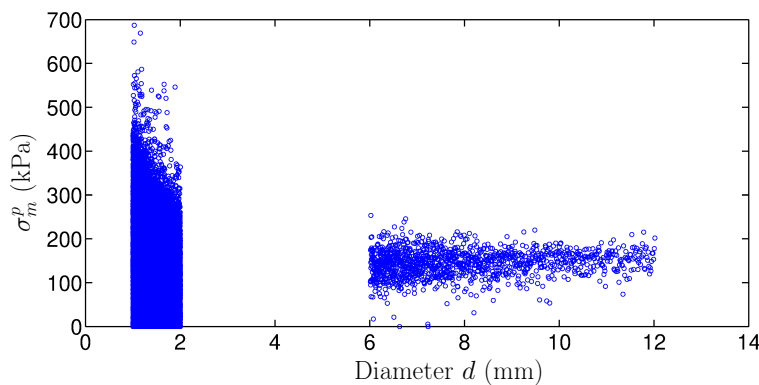
particles in the volume under consideration. The mean internal moment m^p is defined as the trace of the tensor \mathbf{M}^p :

$$m^p = \sum_{k \in p} \mathbf{f}^k \cdot \mathbf{r}^k, \quad (5)$$

where (\cdot) denotes the dot product between two vectors. Scholtès et al. [22] considered the mean internal moment m^p as a degree of interlocking for the particle under consideration: the higher the mean internal moment m^p is, the less the particle is susceptible to be detached by seepage flow.



(a)



(b)

Figure 7: (a) Mean internal moment m^p and (b) mean stress σ_m^p versus the diameter d for the particles in the sample with $f_c = 30\%$ at the initial state

As can be seen in Equation (5), the mean internal moment m^p depends on the particle radius r and the magnitude of the contact force \mathbf{f}^k which tends, in turn, to decrease as the particle size decreases. Indeed, Voivret et al. [27] found that the larger particles tend to carry stronger forces, whereas the smaller particles tend to carry weaker forces. As a result, m^p tends to decrease as the particle size decreases as shown in Figure 7.a. One might consider the stress tensor $\boldsymbol{\sigma}^p = \mathbf{M}^p/V^p$ defined for each particle (V^p is the volume of the particle) to assess its degree of interlocking. Peters et al. [17] used the mean stress $\sigma_m^p = \text{tr}(\boldsymbol{\sigma}^p) = m^p/V_p$ to separate the chain of strongly stressed particles from the chain of weakly stressed particles. Like the mean

internal moment m^p , the mean stress σ_m^p is dependent upon the particle size: it tends to scale down with the particle size as shown in Figure 7.b.

Scholtès et al. [22] assumed that the particle having the smallest value of the mean internal moment m^p is the most likely erodible; therefore, this particle is removed from the sample. After each particle removal, the sample is brought to the equilibrium before removing the next erodible particle. As mentioned above, the mean internal moment is dependent upon the particle size. As a result, this criterion might remove the finest particles in the solid skeleton. In the next section, we will propose a new method to identify the loose particles based on the force networks.

4.2. Method based on the force networks

Radjai et al. [18] distinguished two force networks, namely weak and strong force networks, which are composed of the contacts where the force magnitude f^k is smaller and bigger than the average value \bar{f} , respectively. The authors found that the strong network sustains almost the shear stress, whereas the weak network behaves like a liquid without bearing significant shear stress. The former constitutes, therefore, the solid skeleton of the granular assembly. We assume that a particle belongs to this solid skeleton if the strong force network passes through it – in other words, it has at least two contacts in the strong force network. Furthermore, all the particles that do not belong to the solid skeleton are loose ones as illustrated in Figure 8.

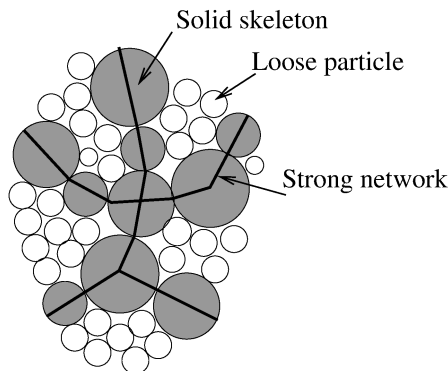


Figure 8: Illustration of the solid skeleton (gray particles) and the loose fraction (white particles) in a granular assembly.

Figure 9 shows the contributions of the solid skeleton and of the loose fraction to the macroscopic mean and deviatoric stresses, p and q , at the peak state versus fine content f_c . This figure confirms that the solid skeleton identified by this method carries primarily stresses. Moreover, the loose fraction carries a small part of the mean stress but a negligible part of the deviatoric stress. Table 4 presents the percentages by mass of the fine and coarse particles in the loose fraction for different fine contents f_c at the initial state (isotropic stress state). These percentages are calculated with respect to the total solid mass of all particles.

This table shows that the loose fraction includes a major fraction of the fine particles but a small fraction of the coarse particles. More precisely, almost all of the fine particles are loose for $f_c \leq 20\%$. Starting from 20% of fine content, more and more fine particles participate in carrying the stresses and then take part in the *solid skeleton*. Almost all the coarse particles are included in the solid skeleton when $f_c > 20\%$ – in other words, the loose fraction contains almost only fine particles.

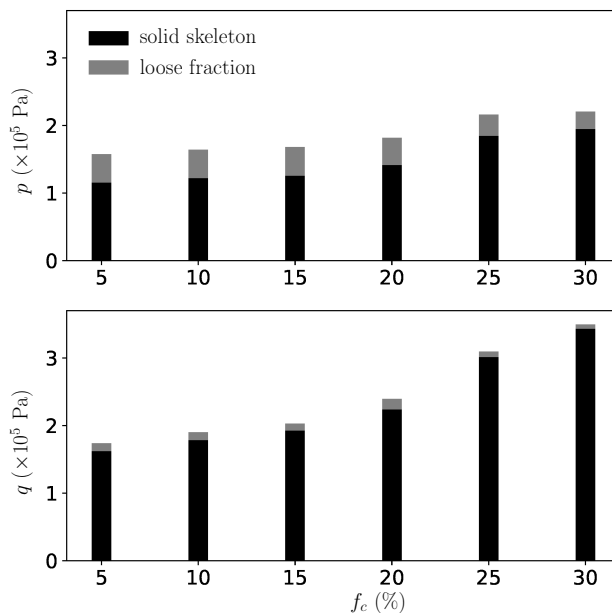


Figure 9: Contributions of the solid skeleton and of the loose fraction to the mean stress p and deviatoric stress q at the peak state versus fine content f_c .

Table 4: Percentages by mass of the fine and coarse particles in the loose fraction for different fine contents f_c at the initial state.

f_c	% of loose fines	% of loose coarses
5%	5.0%	26.0%
10%	10.0%	29.3%
15%	15.0%	23.0%
20%	20.0%	20.3%
25%	24.13%	1.0%
30%	22.0%	0.1%

We assume that the particles belonging to the solid skeleton are non-erodible and only the fine particles in the loose fraction are erodible. Furthermore, the degree of interlocking of each fine loose particle depends on its coordination number (the number of contacts with its neighbors). At each removal step, a fraction $\Delta\mu_e$ of the fine loose particles that have the lowest coordination number is removed. After that, the sample

is stabilized until it reaches a new equilibrium, and the solid skeleton and the loose fraction are updated. This removal procedure is repeated until reaching the target eroded mass μ_e . Like for the random removal procedure presented in Section 3, the removal rate $\Delta\mu_e$ has little effect on the mechanical behavior of the eroded sample; as a result, $\Delta\mu_e = 1\%$ is used to remove erodible particles. In the next section, the behaviors of samples eroded by the two methods presented in the current section and by the random removal method presented in Section 3 will be compared.

5. Comparison between different removal methods

Let us first compare the three aforementioned removal methods in terms of rearrangement of particles triggered by the loss of fine particles. Figure 10 presents the volumetric strain ε_v induced by the three particle removal methods versus the eroded mass μ_e for the sample with $f_c = 30\%$. It is shown that all the three methods leads to a contraction of the eroded sample under constant isotropic stress state. Scholtès et al. [22] found that the particle removal leads actually to a contraction at low values of the stress ratio q/p but to a dilation at high values of q/p . The random removal method disturbs the most the sample, leading to the highest contraction. This is due to the fact that the fine particles belonging to the solid skeleton are also removed by this method, leading to a collapse of the solid skeleton and thus a great rearrangement of particles. On the other hand, given that only fine particles in the loose fraction are removed, the method based on the force networks induces the lowest contraction to the sample, meaning that the solid skeleton is the less disturbed by the particle removal. The method of Scholtès et al. and the method based on the force networks give almost the same results for $\mu_e \leq 20\%$ but different results for $\mu_e > 20\%$.

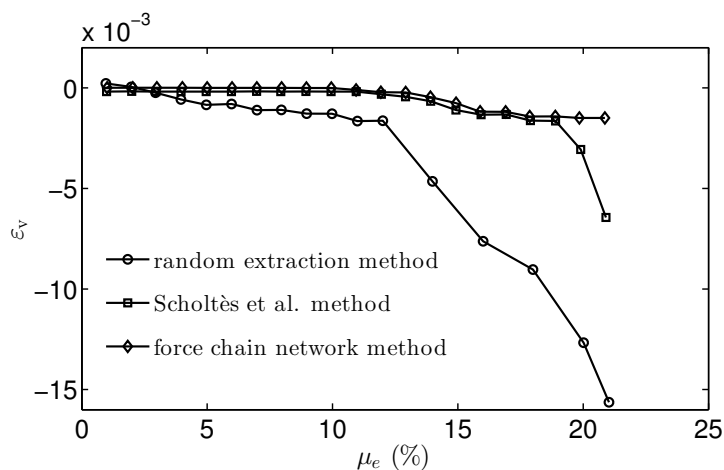


Figure 10: Variation of the volumetric strain ε_v versus the eroded mass μ_e induced by the three different removal methods.

Figure 11 shows the stress-strain behavior of the samples eroded by the three methods. The original sample with fine content of 30% is eroded at the initial state with eroded masses $\mu_e = 10\%$ and 20%. This

figure indicates clearly the importance of a criterion to remove fine particles. One can see that the method of Scholtès et al. gives results close to those given by the random removal method. The behaviors of the samples eroded by these methods are strongly degraded in comparison with that of the original sample. This result means that, like the random removal method, the method of Scholtès et al. removes fine particles in the solid skeleton, leading to a great degradation of the mechanical behavior of the eroded sample. The method based on the force networks leads also to a reduction in the shear strength and in the dilatancy of the eroded sample. However, this degradation is less marked than that induced by the two other methods. Indeed, with the same eroded mass $\mu_e = 20\%$, the shear strength at the peak state of the eroded samples given by the method of Scholtès et al. and the random removal method is reduced by about 55%, whereas a reduction of 28% is observed for the method based on the force networks. In addition, the difference in the behavior of the eroded samples given by the three methods increases with the eroded mass μ_e . It is interesting to note that all the three methods lead to almost the same shear strength at the critical state. This result indicates that the concept of the critical state is still valid for eroded soils. As long as the grain size distribution and the particle properties of the soil are preserved, any modification of the initial microstructure or density leads to the same shear strength of the soil at the critical state.

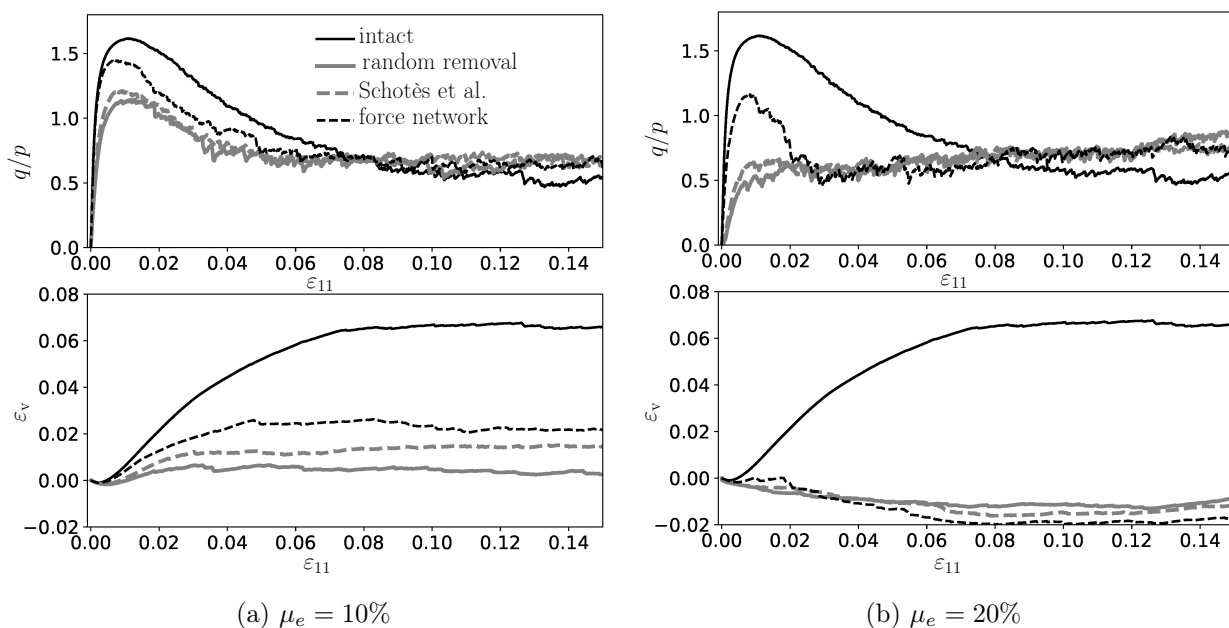


Figure 11: Stress ratio q/p and volumetric strain ε_v versus axial strain ε_{11} for the eroded samples with (a) 10% and (b) 20% of fine particles removed from the original sample $f_c = 30\%$ using different removal methods.

One might think that the degradation of the mechanical properties of an eroded soil is mainly due to an increase in the void ratio induced by the internal erosion; therefore, its mechanical behavior can be studied by simply reconstituting a sample with the same void ratio as that of the eroded one. Table 5

presents the void ratio e of the eroded samples obtained with the three methods. It is shown that the method of Scholtès et al. and the one based on the force networks give both the same void ratio after the particle removal. However, the mechanical behaviors of the eroded samples given by these two methods are completely different as shown in Figure 11. In addition, the eroded sample given by the random removal method has significantly lower void ratio but it has much lower shear strength at the peak state than that of the eroded sample given by the method based on the force networks. These results mean that not only the void ratio but also the microstructure are determinant for the mechanical behavior of eroded soils; and a sample reconstitution is not relevant to study their mechanical behavior. Furthermore, the above results indicate that the experimental technique of Chen et al. [5] based on the salt dissolution would be not relevant as well since it would lead to a greater disturbance of the microstructure of the soil than that caused by the internal erosion which tends to wash out only particles carrying no or little stresses.

Table 5: Initial global void ratio e of the eroded samples obtained with different removal methods from the original sample with $f_c = 30\%$.

Method	$\mu_e = 10\%$	$\mu_e = 20\%$
Method of Scholtès et al.	0.43	0.60
Random removal	0.42	0.57
Method based on the force networks	0.43	0.60

At the micro-scale, the way of removing fine particles has a great impact on the stresses carried by fine and coarse fractions. As mentioned in Section 3, for a fine content $f_c \leq 30\%$, the fine particles have a small contribution towards carrying the macroscopic stresses but they bring a great bracing effect to the solid skeleton which is primarily constituted of coarse particles. As a consequence, a removal of fine particles destabilizes this solid skeleton, leading to a reduction in the capability of the coarse fraction to carry stresses. Figure 12 shows the mean and deviatoric stresses, \hat{p}^C and \hat{q}^C , carried by the coarse fraction at the peak and critical states in the samples eroded by the three methods with different eroded masses μ_e , in comparison with those obtained for the original sample with $f_c = 30\%$. It is clear that the reduction in stresses carried by the coarse fraction at the peak state depends strongly on how fine particles are removed (Figure 12.a). By removing only fine particles in the weak force network, the reduction in stresses carried by the coarse fraction at the peak state is significantly less marked than that caused by the random removal method or by the method of Scholtès et al. In addition, this difference is much clearer for the deviatoric stress than for the mean stress. This result confirms that the removal method based on the force networks leads to a lower disturbance of the solid skeleton of the eroded sample than that caused by the two other methods. On the contrary, the stresses carried by the coarse fraction at the critical state are almost independent of the way that fine particles are removed (Figure 12.b), in comparison with those at the peak state. This explains why the shear strength of eroded samples at the critical state is almost the same for all the three particle

removal methods as shown in Figure 11.

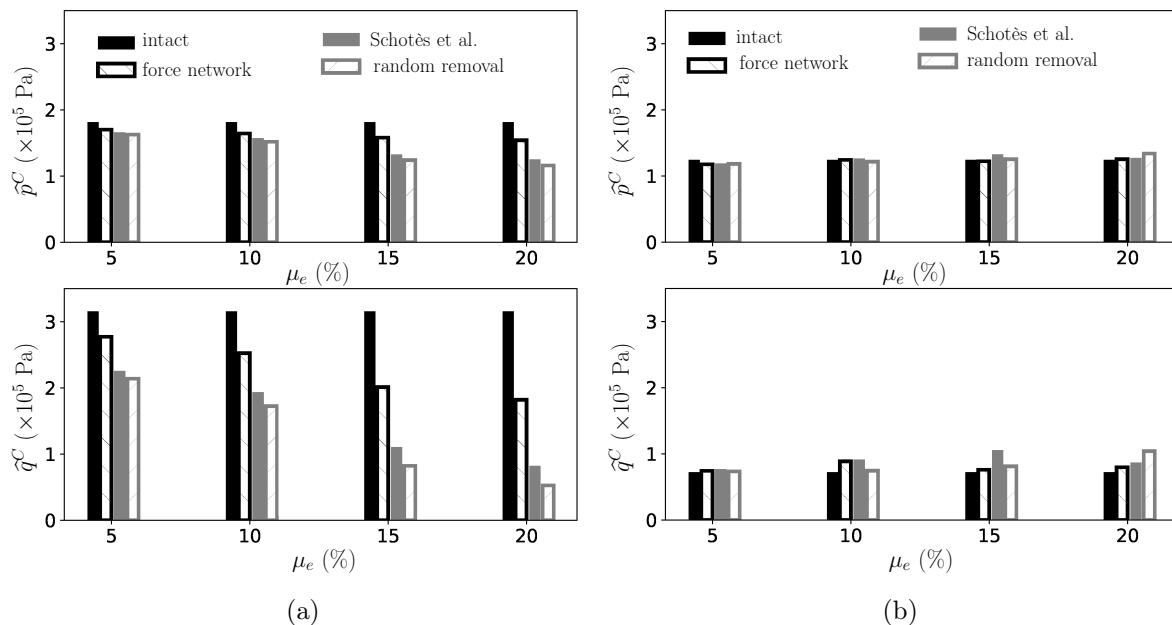


Figure 12: The mean and deviatoric stresses \hat{p}^C and \hat{q}^C carried by the coarse fraction versus the eroded mass μ_e for the eroded samples given by the three methods, compared to those of the intact sample with $f_c = 30\%$: (a) at the peak state and (b) at the critical state.

6. Conclusions

In this paper, we present a study of consequences of a loss of fine particles on the mechanical behavior of granular soils by using the DEM. Gap-graded samples with different fine contents f_c were simulated. Three different particle removal methods were adopted to produce eroded samples. The first method consists in removing randomly fine particles, while the two other ones remove fine particles that are weakly stressed. The method of Scholtès et al. [22] identifies these particles by using the mean internal moment m^p . However, this measure was found to have a size effect as it tends to scale up with the particle size. As a consequence, finest particles belonging to the solid skeleton might be removed since they have small values of m^p . To remediate this drawback, we proposed a new method to identify these fine loose particles by using the concept of the weak and strong force networks proposed by Radjai et al. [18]. Moreover, instead of removing fine particles one by one, a package of fine particles with a given mass fraction $\Delta\mu_e$, called *removal rate*, is removed at each removal step to gain the computation time. It was found that this removal rate has little effect on the mechanical behavior of eroded samples.

The random removal method is similar to the experimental tests performed by Chen et al. [5] who replaced a fraction of fine particles by salt and then dissolved salt by water under constant stresses. A

removal of fine particles does not have a significant effect on the shear strength for samples with low fine contents ($f_c < 20\%$) but have a great effect for samples with higher fine contents. This numerical finding is qualitatively in good agreement with the experimental finding of Chen et al. A micro-mechanical investigation into stresses carried by the coarse and fine fractions pointed out that the fine particles have a small contribution towards carrying stresses but they serve as a bracing system to stabilize laterally the coarse fraction for a fine content $\geq 20\%$, allowing the latter to carry great stresses. As a consequence, a removal of fine particles destroys this bracing system, leading to a reduction in the capability of the coarse fraction to carry stresses, particularly the deviatoric stress.

By identifying particles belonging to the weak and strong force networks, a loose fraction containing the weakly stressed particles was separated from those in the solid skeleton that carries mainly stresses, particularly the deviatoric stress. The loose fraction includes a major part of fine particles, whereas the solid skeleton includes a major part of coarse particles. A removal of fine particles in the loose fraction triggers a contraction under a constant isotropic stress. Nevertheless, this contraction is much less marked than that triggered by the random removal. In addition, the mechanical behavior of the sample eroded by the former method is much less impacted than that obtained with the latter method. The method of Scholtès et al. gives results quite similar to those given by the random removal method, meaning that the mean internal moment m^p might not be adequate to characterize the level of interlocking of fine particles. From a micro-mechanical point of view, a removal of fine particles in the loose fraction was found to degrade less the bearing capability of the solid skeleton than a random removal. This study also showed that the mechanical behavior of an eroded soil cannot be accurately studied by simply reconstituting a sample with the same void ratio as that of the eroded one or by a technique similar to the one used by Chen et al. since it depends strongly on the microstructure induced by the internal erosion.

A fully coupled DEM-CFD model is still computationally very expensive to simulate the whole suffusion process that occurs in the granular soils with gap-graded or upwardly concave grain size distributions. Therefore, the particle removal approach appears to be a good alternative. This study pointed out the importance of a criterion to identify the particles to be removed. The criterion proposed in the current paper seems to be a good candidate to mimic the fact that the seepage flow erodes selectively fine particles that carry no or little stresses. The accuracy of this criterion needs to be further studied by comparing the internal state of an eroded soil given by this criterion with that given by a fully coupled DEM-CFD model. Moreover, the self-filtration of detached fine particles by the solid skeleton needs to be taken into consideration to describe more precisely the suffusion. To do so, the pore network of the solid skeleton can be characterized by using a method based on the Delaunay triangulation [16]. The detached fine particles can be transported from one pore to another and can be trapped by constrictions smaller than their size.

7. Acknowledgements

The authors would like to thank Cedre program of the French and Lebanese scientific cooperation for the financial support for this research project.

References

- [1] Aboul-Hosn, R.: Suffusion and its effects on the mechanical behavior of granular soils: numerical and experimental investigations. Ph.D. thesis, Grenoble Alpes (2017)
- [2] Chang, D., Zhang, L.: A stress-controlled erosion apparatus for studying internal erosion in soils. *Geotechnical Testing Journal* **34**(6), 579–589 (2011)
- [3] Chang, D., Zhang, L.: Extended internal stability criteria for soils under seepage. *Soils and Foundations* **53**(4), 569–583 (2013)
- [4] Chareyre, B., Cortis, A., Catalano, E., Barthélemy, E.: Pore-scale modeling of viscous flow and induced forces in dense sphere packings. *Transport in Porous Media* **94**(2), 595–615 (2012)
- [5] Chen, C., Zhang, L., Chang, D.: Stress-strain behavior of granular soils subjected to internal erosion. *Journal of Geotechnical and Geoenvironmental Engineering* **142**(12), 06016,014 (2016)
- [6] Froiio, F., Callari, C., Rotunno, A.F.: A numerical experiment of backward erosion piping: kinematics and micromechanics. *Meccanica* **54**(14), 2099–2117 (2019)
- [7] Hicher, P.Y.: Modelling the impact of particle removal on granular material behaviour. *Géotechnique* **63**(2), 118–128 (2013)
- [8] Hosn, R.A., Benahmed, N., Nguyen, C.D., Sibille, L., Philippe, P., Chareyre, B.: Effects of suffusion on the soil’s mechanical behavior: Experimental investigations. In: *European Working Group on Internal Erosion*, pp. 3–15 (2018)
- [9] Hu, Z., Zhang, Y., Yang, Z.: Suffusion-induced deformation and microstructural change of granular soils: a coupled CFD–DEM study. *Acta Geotechnica* **14**(3), 795–814 (2019)
- [10] Kawano, K., Shire, T., O’Sullivan, C.: Coupled particle-fluid simulations of the initiation of suffusion. *Soils and Foundations* **58**(4), 972–985 (2018)
- [11] Ke, L., Takahashi, A.: Experimental investigations on suffusion characteristics and its mechanical consequences on saturated cohesionless soil. *Soils and Foundations* **54**(4), 713–730 (2014)
- [12] Kenney, T., Lau, D.: Internal stability of granular filters. *Canadian Geotechnical Journal* **22**(2), 215–225 (1985)
- [13] Lominé, F., Scholtès, L., Sibille, L., Poullain, P.: Modeling of fluid–solid interaction in granular media with coupled lattice Boltzmann/discrete element methods: application to piping erosion. *International Journal for Numerical and Analytical Methods in Geomechanics* **37**(6), 577–596 (2013)
- [14] Moreau, J.: Numerical investigation of shear zones in granular materials. In: *Friction, Arching, Contact Dynamics*, pp. 233–247. World Scientific, Singapore (1997)
- [15] Nguyen, C.D., Benahmed, N., Andò, E., Sibille, L., Philippe, P.: Soil microstructural changes induced by suffusion: x-ray computed tomography characterization. In: *E3S Web of Conferences*, vol. 92, p. 01010 (2019)
- [16] Nguyen, N.S., Taha, H., Marot, D.: A new Delaunay triangulation-based approach to characterize the pore network in granular materials. *Acta Geotechnica* pp. 1–19 (2021)
- [17] Peters, J., Muthuswamy, M., Wibowo, J., Tordesillas, A.: Characterization of force chains in granular material. *Physical Review E* **72**(4), 041,307 (2005)
- [18] Radjai, F., Wolf, D.E., Jean, M., Moreau, J.J.: Bimodal character of stress transmission in granular packings. *Physical Review Letters* **80**(1), 61 (1998)

- [19] Robinson, M., Luding, S., Ramaioli, M.: SPH-DEM simulations of grain dispersion by liquid injection. In: AIP Conference Proceedings, vol. 1542, pp. 1122–1125 (2013)
- [20] Rousseau, Q., Sciarra, G., Gelet, R., Marot, D.: Modelling the poroelastoplastic behaviour of soils subjected to internal erosion by suffusion. *International Journal for Numerical and Analytical Methods in Geomechanics* **44**(1), 117–136 (2020)
- [21] Sail, Y., Marot, D., Sibille, L., Alexis, A.: Suffusion tests on cohesionless granular matter. *European Journal of Environmental and Civil Engineering* **15**(5), 799–817 (2011)
- [22] Scholtès, L., Hicher, P.Y., Sibille, L.: Multiscale approaches to describe mechanical responses induced by particle removal in granular materials. *Comptes Rendus Mécanique* **338**(10-11), 627–638 (2010)
- [23] Seblany, F., Vincens, E., Picault, C.: Determination of the opening size of granular filters. *International Journal for Numerical and Analytical Methods in Geomechanics* (2021)
- [24] Sterpi, D.: Effects of the erosion and transport of fine particles due to seepage flow. *International Journal of Geomechanics* **3**(1), 111–122 (2003)
- [25] Taha, H., Nguyen, N.S., Marot, D., Hijazi, A., Abou-Saleh, K.: Micro-scale investigation of the role of finer grains in the behavior of bidisperse granular materials. *Granular Matter* **21**(2), 28 (2019)
- [26] Tran, D., Prime, N., Froio, F., Callari, C., Vincens, E.: Numerical modelling of backward front propagation in piping erosion by DEM-LBM coupling. *European Journal of Environmental and Civil Engineering* **21**(7-8), 960–987 (2017)
- [27] Voivret, C., Radjai, F., Delenne, J.Y., El Youssoufi, M.S.: Multiscale force networks in highly polydisperse granular media. *Physical Review Letters* **102**(17), 178,001 (2009)
- [28] Šmilauer, V., et al.: Yade Documentation 2nd ed. The Yade Project (2015). DOI 10.5281/zenodo.34073. <http://yade-dem.org/doc/>
- [29] Wan, C., Fell, R.: Assessing the potential of internal instability and suffusion in embankment dams and their foundations. *Journal of Geotechnical and Geoenvironmental Engineering* **134**(3), 401–407 (2008)
- [30] Wood, D., Maeda, K.: Changing grading of soil: effect on critical states. *Acta Geotechnica* **3**, 3–14 (2008)
- [31] Wood, D., Maeda, K., Nukudani, E.: Modelling mechanical consequences of erosion. *Géotechnique* **60**(6), 447–457 (2010)
- [32] Zhao, J., Shan, T.: Coupled CFD–DEM simulation of fluid–particle interaction in geomechanics. *Powder Technology* **239**, 248–258 (2013)